Journal of Information Hiding and Multimedia Signal Processing ©2015 ISSN 2073-4212
Ubiquitous International Volume **6**, Number **2**, March **2015**

Segmentation of Median Nerve by Greedy Active Contour Detection Framework on Strain Ultrasound Images

You-Wei Wang[1], Chii-Jen Chen[2,*], Sheng-Fang Huang[3], and Yi-Shiung Horng[4,5]

[1]Department of Computer Science and Information Engineering
National Taiwan University, Taipei, Taiwan

[2,*]Department of Computer Science and Information Engineering
Yuanpei University of Medical Technology, Hsinchu, Taiwan
Corresponding author: cjchen@mail.ypu.edu.tw

[3]Department of Medical Informatics
Tzu Chi University, Hualien, Taiwan

[4]Department of Physical Medicine and Rehabilitation
Taipei Tzu Chi Hospital, Buddhist Tzu Chi Medical Foundation, Taipei, Taiwan
[5]Department of Medicine
Tzu Chi University, Hualien, Taiwan

Received November 2014; revised December 2014

Abstract. *Carpal tunnel syndrome (CTS) is commonly occurred in occupations using vibrating manual tools or handling tasks with highly repetitive and forceful manual exertion. Recently, the ultrasonography has been used to evaluate CTS by monitoring median nerve movements. In order to facilitate the automatic segmentation of shape characteristics for the median nerve, this paper designed a framework that used greedy active contour detection (GACD) model to extract the median nerve in ultrasound images. We first selected a ROI to be an initial of virtual contour for median nerve in original ultrasound slice, and then proposed GACD method was used to detect the contour of median nerve. In the experiment, the results show that the performance of the method is feasible and accurate.*
Keywords: Ultrasound, Carpal tunnel syndrome (CTS), Median nerve, Greedy, Active contour.

1. **Introduction.** Carpal tunnel syndrome (CTS) is a clinical disorder caused by compression of the median nerve at the wrist, which is commonly occurred in occupations using vibrating manual tools or handling tasks with highly repetitive and forceful manual exertion. The diagnosis of carpal tunnel syndrome (CTS) can rely on a combination of characteristic symptoms and electrophysiologic abnormalities. Nevertheless, an electrodiagnostic study remains an expensive and time-consuming procedure not readily accessible to many physicians who are encountering the disease.

In recent years, ultrasound imaging plays an important role in the diagnosis of CTS, because of its wide availability, lower cost, non-invasiveness, and shorter examination time [1]. Ultrasound has been shown to have a sensitivity as high as 94% and a specificity as high as 98% in the diagnosis of CTS, and can provide structural abnormalities and diagnostic reference in imaging [2, 3, 4], to make up for the lack of nerve electrical

inspection. Many scholars have been trying to establish the ultrasound diagnostic criteria for the diagnosis of carpal tunnel syndrome and its use, including the measurement of median nerve cross-sectional area, flattening ratio, swelling ratio and palmar bowing of the flexor retinaculum, etc [5]. Dlley et al. used the cross-correlation between the images based on the wrists, elbows, shoulders and neck stretches, to measure the sliding elastic characteristics of the median nerve [6]. On the other hand, Yoshii et al. estimated the cross-sectional area of the median nerve, block aspect ratio, circularity, block perimeter and other characteristics, and then judge the differences and effectiveness of these features [7].

In order to facilitate the automatic extraction of shape characteristics for the median nerve, this paper presents a greedy active contour detection (GACD) framework to detect the contour of median nerve on strain sonographic images. We first chose a ROI to be an initial of virtual contour of median nerve in original image slice. This pre-processing can enhance the sensitivity of region contour, and assist to detect the contour of median nerve by proposed GACD method. Finally, a convergent condition is used to stop the proposed GACD procedure when the contour of median nerve is found. In the experiment, the results show that the performance of the method is feasible and accurate.

2. **Data Acquisition.** In this paper, there are 12 testing data which were supported by Department of Physical Medicine and Rehabilitation, Taipei Tzu Chi Hospital, Buddhist Tzu Chi Medical Foundation, Taipei, Taiwan. In each case, there are 220 continuous imaging slices and the scanning time is 20 seconds per case. The size of each imaging slice is 352*434 pixels. During the scanning procedure, six wrist motions, which include rest, straight, hook, fist, tabletop, and straight fist, must be completed by each patient within the time, as shown in Figure 2. Then, the median nerve will be tightened and relaxed by the six wrist motions at different time points, and displayed in the continuous imaging slices. After the data acquisition, the contour of median nerve can be obtained by the proposed curve matching algorithm from the continuous imaging slices.

FIGURE 1. The first five wrist motions are straight, hook, fist, tabletop, and straight fist. The final one, straight fist, is a motion simply for taking a rest break.

3. **Segmentation of Median Nerve by GACD Framework.** In this section, we designed a segmentation framework that used greedy active contour detection (GACD) model to extract the edge of median nerve in ultrasound images. Because the noise and speckle are always existed in ultrasound image, we have to apply some pre-processing method to reduce noise and enhance contrast for the region of interest (ROI). We used ROI to be an initial of virtual contour of median nerve in ultrasound image. The pre-processing can enhance the sensitivity of GACD to detect the contour of median nerve.

Through the mechanism of convergence, we can obtain the contour of median nerve, and the system framework is shown in Figure 1.

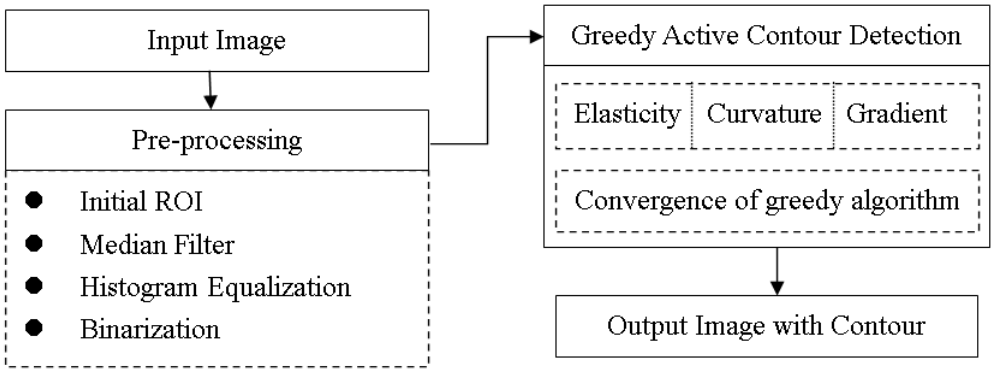

FIGURE 2. The system framework of median nerve segmentation.

3.1. **Pre-processing for Contour Initialization.** In this sub-section, we briefly introduce the main purpose of pre-processing for contour initialization. At the beginning of system processing, in order to assist the contour segmentation by proposed greedy active contour detection (GACD) model, we would select a region of interest (ROI) to be the initial contour of median nerve. The corresponding control points on this initial contour can also be generated to assist the computation of GACD framework, as shown in Figure 3. However, because the ultrasound images have high noise, we used median filter to decrease the pepper or salt noises in the ROI. Then, the ultrasound images are also low contrast, and we used histogram equalization to improve the low contrast problem. Histogram equalization can enhance the contrast that means the ambiguous of ROI can be a higher than contrast image. Finally, we transferred the ROI to a binary image, and the gradient of ROI can be more easily to calculate with binary image.

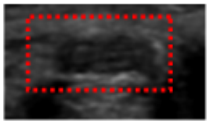

FIGURE 3. The initial contour of ROI.

3.2. **Greedy Active Contour Detection Method.** The proposed contour detection method, greedy active contour detection (GACD), can be divided into three parts: elasticity (Ela), curvature (Cur), Gradient (Gra) [8]. The main idea of GACD method is from the active contour model (ACM), which can control the initial contour to shrink to the contour [9, 10, 11]. These criteria can assist the GACD algorithm to compute the distance, curve, and boundary of region contour by the limitation of control points. The contour detection will be able to define the target contour that formula as following [8]:

$$GACD = argMIN(Ela + Cur + Gra) \tag{1}$$

where Ela is used to decide the distance between all control points of ROI. Cur is able to regulate the degree of bending, to limit the curve. Gra means the gradient of

image that can find out the most likely contour points as GACD. We used three criteria to decide the control points of ROI to shrink the contour in different iterations. The above formula is used to search each control point around the 3*3 mask/kernel that we can choose the argument of minimum GACD to be the control points in next iteration. Then after several iteration of GACD, the contour will be shrunk on the boundary of median nerve. In other words, the control points moved with 3*3 mask/kernel in each iteration to decide their direction of movement, as shown in Figure 4, and P is the set of control points. During each iteration, the distances between different control points would be examined. If two control points are too closed, this two control points would be removed, and new control point would be created at the center between original two closed control points. If the distance of control point is too far for its adjacent control points, we will add the center point between this two adjacent control points that can reduce the program to repeat the calculation of control points.

In elasticity (Ela) part, the adjacent control points are used to decide elasticity that can limit the distance of the control points with each other. The corresponding formulas are calculated as following:

$$\bar{d} = \frac{|p_N - p_1| + \Sigma_{i=1}^{N-1}|p_{i+1} - p_i|}{N} \tag{2}$$

$$Ela = |\bar{d} - |p_i - p_{i-1}|| \tag{3}$$

where $\bar{d}$ is the average distance of all control points. Ela is the average distance between control points to decide the best locational choice of movement [12], and to limit the distance of control points. In other words, Ela can obtain the more suitable distance between each control point.

In curvature (Cur) part, the adjacent control points are used to regulate the bending degree that can decide the curve with two neighboring control points, defined as following:

$$Cur = |(p_{i+1} - p_i) + (p_{i-1} - p_i)|^2 \tag{4}$$

where p_i is the control point. In previous formula, p_i is the target control point to compare with two neighbors of control points, such as p_{i-1} is p_{i+1}, to decide the bending condition. Figure 5 is a schema of curvature. When Cur of p_i has large value, it means the curve is not smooth. We hope the bending degree is limited as well as smooth boundary; therefore, the value of Cur is as small as possible [13].

Gradient (Gra) is always used to detect the edge of image region, and also used to differentiate of discrete domain, such as Sobel and Prewitt filters, to obtain the region edge [14, 15]. We used the differential method to compute the gradient value, and the gradient may be the evidence of contour, defined as following:

$$g(x, y) = \sqrt{(I(x+1, y) - I(x, y))^2 + (I(x, y+1) - I(x, y))^2} \tag{5}$$

where $I(x, y)$ is the intensity of image on coordinate (x, y). Then we normalized the gradient such as:

$$Gra = \frac{max(g) - g(p_i)}{max(g) - min(g)} \tag{6}$$

where Gra is the normalized of gradient, $max(g)$ is the maximum gradient in ROI, $min(g)$ is the minimum gradient in ROI. Through the normalization of $g(x, y)$, if the

value of Gra is become smaller, the control point will be the point on the correct contour. If the value of Gra is become larger, the control point is not the point what we want.

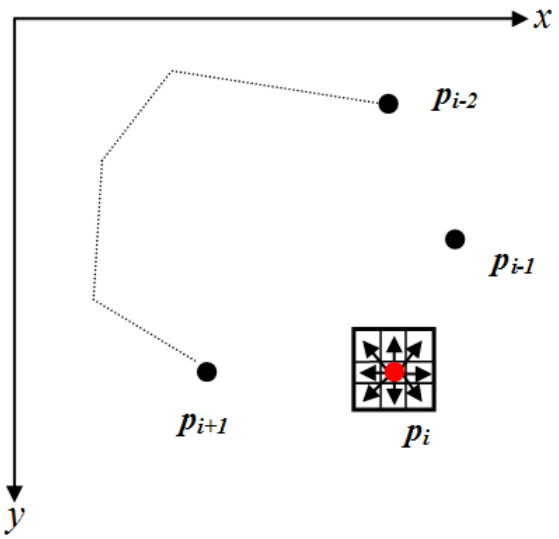

FIGURE 4. The movement of control point.

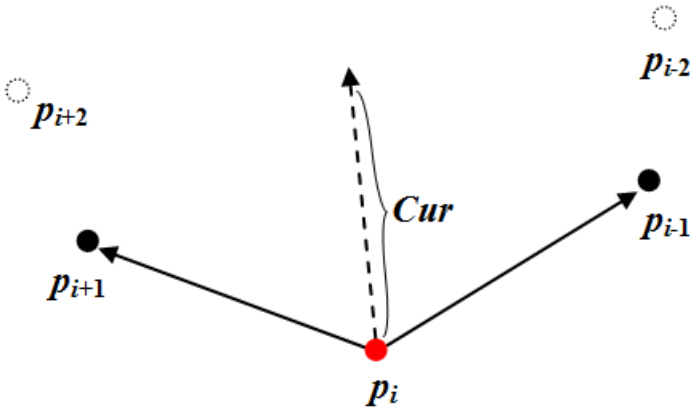

FIGURE 5. A schema of curvature.

3.3. **Convergence of GACD Algorithm.** Finally, the convergent condition of proposed GACD algorithm is required to inform the system that we find the contour of median nerve. In the proposed framework, the control points can be stopped with three criteria of GACD method. When the contour does not change in next iteration that means the contour of median nerve is obtained, as shown in Figure 6. At the end of this step, all control points will be connected to a closed contour, and it will be the contour of median nerve. Overall, the detail procedure proposed GACD method for segmentation of median nerve is shown in Figure 7.

4. **Experimental Result.** In the experiments, there are 12 strain ultrasound cases of median nerve, and 220 imaging slices in each case. For each testing case, the initial ROI and corresponding control points were prepared to be an initial contour of median nerve. According to the computations of Ela, Cur and Gra, the control points of initial contour can be converged by proposed GACD framework after several iterations. For example,

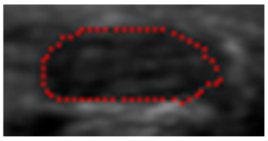

FIGURE 6. The convergence of GACD.

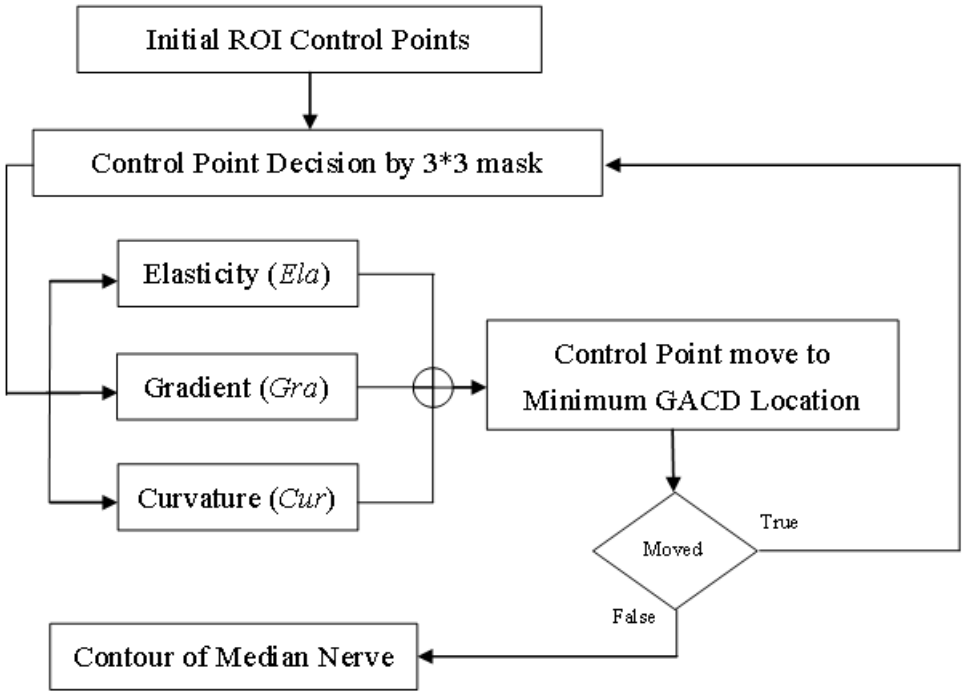

FIGURE 7. The detail of GACD procedure.

the convergent results of proposed GACD procedure in different iterations are shown in Figure 8(a). The degree of convergence for case Figure 8(a) is shown in Figure 8(b); the x-axis is the number of iteration, and y-axis is the convergent degree of contour fetching in each converged round.

In the evaluation of system performance, we used the precision, recall and F-measure to prove the efficiency of proposed GACD framework. In the experiments, the mean values of precision, recall and F-measure can be achieved 85% 91%, 75% 84% and 79% 86% for all testing cases, respectively. The example of segmentation results for median nerve by proposed GACD framework from different cases in a testing case are shown in Figure 9, and the corresponding values of precision, recall and F-measure are shown in Figure 10 (x-axis is the number of testing cases). The higher F-measure is meant that the proposed GACD framework for segmentation of median nerve is practicable.

5. **Discussion and Conclusion.** This paper presents a greedy active contour detection (GACD) procedure to segment the contour of median nerve on strain sonographic images. We first chose a ROI to be an initial of virtual contour of median nerve in original image. This pre-processing can enhance the sensitivity of region contour, and assist to extract the contour of median nerve by proposed GACD framework. A convergent condition is used to stop the proposed GACD procedure when the contour of median nerve is found. The experimental results also show that the performance of the method is feasible and

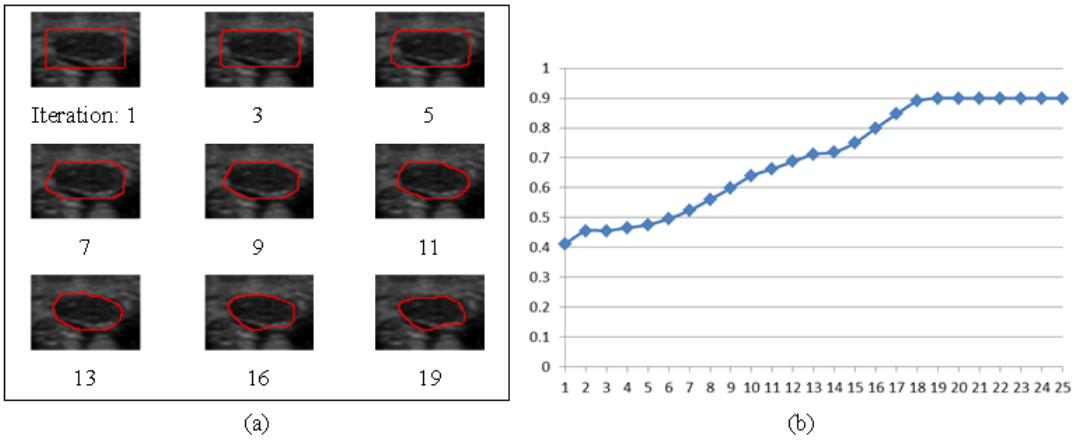

FIGURE 8. The convergent results of proposed GACD procedure in different iterations.

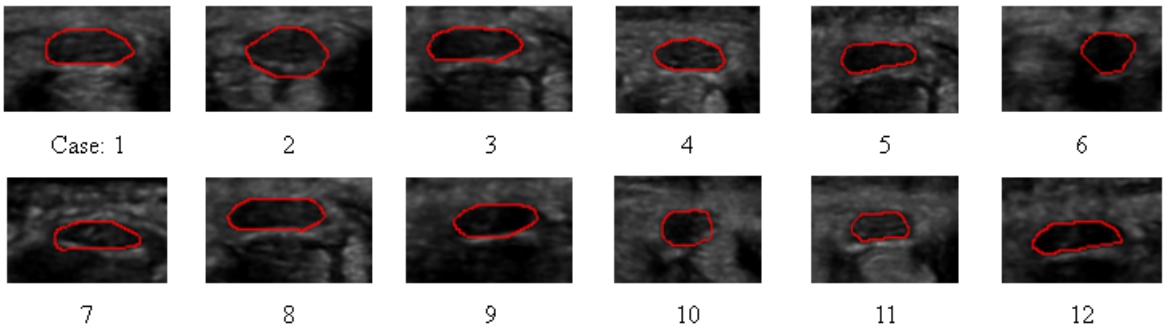

FIGURE 9. The example of segmentation results for median nerve in different cases by proposed GACD framework.

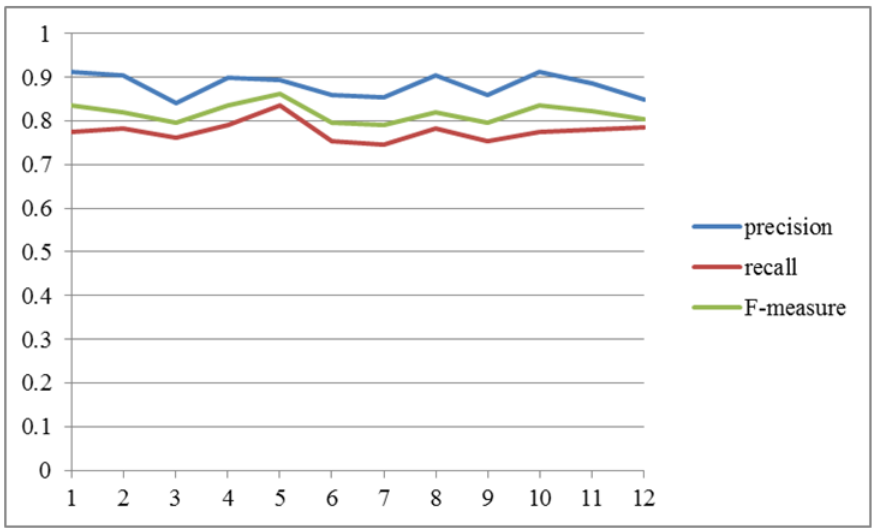

FIGURE 10. The corresponding values of precision, recall and F-measure for all testing cases.

accurate.

However, there are several limitations for the proposed GACD method. The computation of contours is still sensitive to the reference contour. The faulty contour in the reference image may cause the erroneous result of contour segmentation. Therefore, we will improve the method of reference image selection by incorporating with more features in the future. Furthermore, we also need a more robust scheme to correct such erroneous propagation to improve the performance of contour tracking, and provide valuable structural information for the diagnosis of CTS.

Acknowledgment. This work was supported by the Ministry of Science and Technology, Taiwan, under Grant NSC101-2221-E-264-001.

REFERENCES

[1] S.M. Wong, J.F. Griffith, C.F. Hui, S.K. Lo, M. Fu, and K.S. Wong, Carpal Tunnel Syndrome: Diagnostic Usefulness of Sonography, *Radiology*, vol. 232, no. 1, pp. 93-99, 2004.

[2] G.W. Britz, D.R. Haynor, C. Kuntz, R. Goodkin, A. Gitter, and M. Klio, Carpal tunnel syndrome: correlation of magnetic resonance imaging, clinical, electrodiagnostic, and intraoperative findings, *Neurosurgery*, vol. 37, no. 6, pp. 1097-1103, 1995.

[3] I. Duncan, P. Sullivan, and F. Lomas, Sonography in the diagnosis of carpal tunnel syndrome, *AJR Am. J. Roentgenol.*, vol. 173, no. 3, pp. 681-684, 1999.

[4] V. John, H.E. Nau, H.C. Nahser, V. Reinhardt, and K. Venjakob, CT of carpal tunnel syndrome, *AJNR Am. J. Neuroradiol.*, vol. 4, no. 3, pp. 770-772, 1983.

[5] I. Keles, A.T. Karagulle Kendi, G. Aydin, S.G. Zog, and S. Orkun, Diagnostic precision of ultrasonography in patients with carpal tunnel syndrome, *Am. J. Phys. Med. Rehabil.*, vol. 84, no. 6, pp. 443-450, 2005.

[6] A. Dilley, B. Lynn, J. Greening, and N. DeLeon, Quantitative in vivo studies of median nerve sliding in response to wrist, elbow, shoulder and neck movements, *Clin. Biomech.*, vol. 18, no. 10, pp. 899-907, 2003.

[7] Y. Yoshii, H.R. Villarraga, J. Henderson, C. Zhao, K.N. An, and P.C. Amadi, Ultrasound assessment of the displacement and deformation of the median nerve in the human carpal tunnel with active finger motion, *J. Bone Joint Surg. Am.*, vol. 91, no. 12, pp. 2922-2930, 2009.

[8] N.P. Tiilikainen, *A Comparative Study of Active Contour Snakes*, Thesis, Copenhagen University, Denmark, 2007.

[9] D.E. Maroulis, M.A. Savelonas, D.K. Iakovidis, S.A. Karkanis, and N. Dimitropoulos, Variable Background Active Contour Model for Computer-Aided Delineation of Nodules in Thyroid Ultrasound Images, *IEEE Trans. on Information Technology in Biomedicine*, vol. 11, no. 5, pp.537-543, 2007.

[10] H.Y. Lee , N.C. Codella, M.D. Cham, J.W. Weinsaft, and Y. Wang, Automatic Left Ventricle Segmentation Using Iterative Thresholding and an Active Contour Model With Adaptation on Short-Axis Cardiac MRI, *IEEE Trans. on Biomedical Engineering*, vol. 57, no. 4, pp. 905-913, 2010.

[11] A. Mishra and A. Wong, KPAC: A Kernel-Based Parametric Active Contour Method for Fast Image Segmentation, *IEEE Signal Processing Letters*, vol. 17, no. 3, pp. 312-315, 2010.

[12] K.R. Castleman, T.P. Riopka, and W. Qiang, FISH image analysis, *IEEE Engineering in Medicine and Biology Magazine*, vol. 15, no. 1, pp. 67-75, 1996.

[13] D.J. Williams and M. Shah, A fast algorithm for active contours and curvature estimation, *CVGIP: Image Understanding*, vol. 55, no. 1, pp. 14-26, 1992.

[14] S. Arslan, T. Ersahin, R. Cetin-Atalay, and C. Gunduz-Demir, Attributed Relational Graphs for Cell Nucleus Segmentation in Fluorescence Microscopy Images, *IEEE Trans. on Medical Imaging*, vol. 32, no. 6, pp. 1121-1131, 2013.

[15] K. Somkantha, N. Theera-Umpon, and S. Auephanwiriyakul, Boundary Detection in Medical Images Using Edge Following Algorithm Based on Intensity Gradient and Texture Gradient Features, *IEEE Trans. on Biomedical Engineering*, vol. 58, no. 3, pp. 567-573, 2011.